

Pionisation, relativistic lead-lead collisions, and the nature of average phase space density

Bhaskar De^a and S. Bhattacharyya^b

Physics and Applied Mathematics Unit (PAMU), Indian Statistical Institute, Calcutta 700035, India

Received: 14 November 2000 / Revised version: 16 April 2001

Communicated by A. Molinari

Abstract. The average phase space density (APSD) of the particles produced in high energy nuclear collisions at ultrarelativistic energies has here been theoretically estimated on the basis of some particular models for particle production spectra. The model-based values so obtained have been compared with the very recent experimental results in the field on the relevant observable and also with the calculated results obtained by some other models. Based on such comparisons, the present work indicates very strongly that Hagedorn's model has a sound potentiality to achieve a competitive status in its capability to deal with the data on the APSD factor in heavy-ion collisions. The impact and implications of all this have also been emphasised here in the end.

PACS. 25.75.-q Relativistic heavy-ion collisions – 25.75.Gz Particle correlations – 24.10.Pa Thermal and statistical models – 13.85.Ni Inclusive production with identified hadrons

1 Introduction

Pionisation in high energy heavy-ion collisions constitutes an interesting and exciting area for the contemporary studies [1]. Characterising the spatial and dynamical distribution of pions, a particle interferometry-based space-time analysis helps us to estimate the average phase space density [2–4] attained in the collisions. This factor offers a reliable and convenient testing ground for the proposed phenomenological models applied to the microscopic simulations of the complicated multiparticle dynamics. In fact, this factor and the topic thus becomes essentially a linking bridge connecting the physics of relativistic heavy-ion collisions, (lead-lead collisions in the present work), multiparticle production scenario and the physics of quark-gluon plasma (QGP).

The average phase space density (APSD), that is, the phase space density averaged over the homogeneity volume of the particles immediately after the completion of hadronisation called freeze-out, depends mainly on two factors: i) the nature of the single-particle momentum spectrum and ii) the behaviour of the two-particles correlation function. For the former, there are various models among which we choose here a few as stated later and described below, while the latter remains the same throughout the present work. The main objective here is to calculate the average phase space density on the basis of some

standard empirical models for pionisation which accommodate modest observance of Feynman Scaling (FS) in the nucleon-nucleon collision, to modify them necessarily for applying to the cases of nucleus-nucleus collisions and to test the merits of the applied models in the light of the experimental data on the average phase space density (APSD), denoted by $\langle f \rangle$.

The factor essentially deals with the multiplicity distribution in the phase space region. The estimation of the APSD is sensitive to the absolute multiplicity of the particles. Furthermore, it also provides hints to the possible appearance of “overpopulation” in some parts of the phase space. Such cases of overpopulation might lead, in practical terms, to pion-“laser” phenomena etc. For all these reasons, the interest in the average phase space density is now very much on the rise.

The organisation of this work is as follows. In sect. 2 we introduce the basic formalism with familiarisation of the terms used. In sect. 3, we present the outline of the chosen models for pion production spectra in the nucleon-nucleon collisions which provide one of the key foundations of the calculations of the average phase space density. In sect. 4, we present some relevant and detailed information which are to be used in the final calculations of the APSD. Section 5 contains the results of the model-based calculations and analyses. The last section (sect. 6) is reserved for the precise concluding remarks.

^a e-mail: bhaskar_r@www.isical.ac.in^b e-mail: bsubrata@www.isical.ac.in

2 Expression for average phase space density

The expression for the two-particle correlation function [5–7] is given by

$$C(p_1, p_2) = 1 + \frac{|\int d^4x e^{iq \cdot x} S(x, K)|}{\int d^4x S(x, p_1) \int d^4y S(y, p_2)}, \quad (1)$$

where $(q = p_1 - p_2, K = (p_1 + p_2)/2)$. Combining the above expression with that of the one-particle spectrum obtained from

$$E \frac{d^3N}{dp^3} = P_1(p) = \int d^4x S(x, p), \quad (2)$$

$(S(x, p)$ is the single-particle Wigner phase space density of the particle emitting source), we get

$$P_1(p_1)P_1(p_2)[C(p_1, p_2) - 1] = \left| \int d^4x e^{iq \cdot x} S(x, K) \right|^2. \quad (3)$$

Let us introduce the time integrated emission function

$$\Sigma(\mathbf{x}, \mathbf{K}) = \int_{-\infty}^{\infty} dt S(t, \mathbf{x} + \mathbf{v}t, \mathbf{K}), \quad (4)$$

where $\mathbf{v} = \mathbf{K}/K^0$. This quantity allows us to rewrite the integral of eq. (3) over on-shell momenta q satisfying $q \cdot K = 0$,

$$\begin{aligned} & \int d^4q \delta(q \cdot K) [P_1(K + \frac{q}{2})P_1(K - \frac{q}{2})(C(q, K) - 1)] \\ & \approx \frac{(2\pi)^2}{E_K} \int d^3x \Sigma^2(\mathbf{x}, \mathbf{K}). \end{aligned} \quad (5)$$

Here, the on-shell approximation (which is valid for $q^2 \ll 4E_K^2$) has allowed the replacement $K^0 \rightarrow E_K = \sqrt{m^2 + \mathbf{K}^2}$. We also find,

$$P_1(\mathbf{p}) = \int d^3x \Sigma(\mathbf{x}, \mathbf{p}) \quad (6)$$

$\Sigma(\mathbf{x}, \mathbf{p})$ is not the phase space density. In the following, we establish how it is connected to the latter. The phase space density $f(t, \mathbf{x}, \mathbf{p})$ is obtained by summing over all the particles of a given momentum emitted up to time t along a given trajectory

$$f(t, \mathbf{x}, \mathbf{p}) = \frac{(2\pi)^3}{E_p} \int_{-\infty}^t dt' S(t', \mathbf{x} + \mathbf{v}(t-t), \mathbf{p}). \quad (7)$$

The factor in front of the integral assures the correct normalization of f to the number of particles for $t > t_f$, where t_f is the last instant of the freeze-out process. One easily can show that

$$\frac{E_p^n}{(2\pi)^{3n}} \int d^3x f^n(t > t_f, \mathbf{x}, \mathbf{p}) = \int d^3x \Sigma^n(\mathbf{x}, \mathbf{p}). \quad (8)$$

From eq. (5) and eq. (6), then, follows:

$$\begin{aligned} & \int d^4q \delta(q \cdot K) [P_1^2(K)(C(q, K) - 1)] \\ & \approx \frac{E_K}{(2\pi)^3} \int d^3x f^2(t > t_f, \mathbf{x}, \mathbf{K}), \end{aligned} \quad (9)$$

$$P_1(\mathbf{K}) = \frac{E_K}{(2\pi)^3} \int d^3x f(t > t_f, \mathbf{x}, \mathbf{K}). \quad (10)$$

In eq. (9) we have performed the smoothness approximation $P_1(K + \frac{q}{2}) \approx P_1(K - \frac{q}{2}) \approx P_1(K)$. Dividing these two equations (and changing the notation $K \rightarrow p$) we obtain [6, 7]

$$\langle f \rangle(\mathbf{p}) = \frac{\int d^3x f^2(t > t_f, \mathbf{x}, \mathbf{p})}{\int d^3x f(t > t_f, \mathbf{x}, \mathbf{p})}, \quad (11)$$

$$\approx P_1(\mathbf{p}) \int d^4q \delta(q \cdot p) [C(q, p) - 1]. \quad (12)$$

This allows to determine the phase space density of free streaming particles averaged over positions at constant global time, since all quantities on the r.h.s can be measured. Due to Liouville's theorem, the phase space density of free-streaming particles does not change, and hence eq. (12) gives the phase space density averaged along the freeze-out hypersurface.

Indeed, for a hypersurface σ_f , on which the freeze-out process is just completed, and a global time coordinate $t_f(\mathbf{x})$, one can show that

$$\begin{aligned} & E_p \int_{\sigma_t} d^3x f^n(t > t_f, \mathbf{x}, \mathbf{p}) \\ & = \int_{\sigma_f} p^\mu d^3\sigma_\mu(x) f^n(t_f(\mathbf{x}), \mathbf{x}, \mathbf{p}), \end{aligned} \quad (13)$$

where σ_t is the hyper surface given by $t = \text{const} > t_f$ and $d^3\sigma_\mu$ is the infinitesimal normal vector to σ_f . The factor $\mathbf{p} \cdot d^3\sigma$ is known from the formalism of Cooper and Frey and stands for the flux of the particles across σ_f . The relation allows us to rewrite eq. (11) as

$$\langle f \rangle(\mathbf{p}) = \frac{\int_{\sigma_f} \mathbf{p} \cdot d^3\sigma(x) f^2(t_f(\mathbf{x}), \mathbf{x}, \mathbf{p})}{\int_{\sigma_f} \mathbf{p} \cdot d^3\sigma(x) f(t_f(\mathbf{x}), \mathbf{x}, \mathbf{p})}. \quad (14)$$

This is the phase space density averaged over the hypersurface along which the freeze-out is just completed. Equation (14) establishes what can be learnt about the phase space density in a model-independent way. A back extrapolation across the freeze-out boundary is only possible if additional assumptions about the mechanism of particle production are made.

For the two-particle correlation we use the Cartesian parametrisation

$$\begin{aligned} C(\mathbf{q}, \mathbf{p}) - 1 = & \exp[-q_0 R_0^2(\mathbf{p}) \\ & - q_s R_s^2(\mathbf{p}) - q_l R_l^2(\mathbf{p}) - q_0 q_l R_{0l}^2(\mathbf{p})], \end{aligned} \quad (15)$$

where q_i 's are the components of the momentum difference in the out-side-long co-ordinate system and $R_s(\mathbf{p})$, $R_o(\mathbf{p})$, $R_l(\mathbf{p})$ and $R_{ol}(\mathbf{p})$ are the HBT radii. The integration over q in eq. (12) is simple and leads to

$$\langle f \rangle(p_T, Y) = \frac{dN}{dY dM_T dM_T d\phi} \frac{1}{V_{\text{eff}}(p_T, Y)}, \quad (16)$$

with

$$V_{\text{eff}}(p_T, Y) = \frac{M_T \cosh Y}{\pi^{3/2}} R_s(\mathbf{p}) \sqrt{R_o^2(\mathbf{p}) R_l^2(\mathbf{p}) - R_{ol}^4(\mathbf{p})}.$$

A comment is in order here. In reality, a fraction of the observed pions stems from resonance decays after freeze-out. But the pions from long-lived resonances have here been reasonably neglected, since they do not practically contribute to the phase space density at freeze-out, as their arrival is much delayed. However, the role of the pions from the short-lived resonances cannot be overlooked as their neglect might lead to underestimation of pions. This is because of the fact that these decays occur in the spatio-temporal region where the emission of direct pions takes place in profuse number leading to the phenomenon of pionisation in which we are interested here, especially in consideration of the transverse momentum or rapidity region of our interest. In accommodating these features, the expression for average phase space density needs to reckon only a correcting and fractionating factor, $\sqrt{\lambda}$ which has to be introduced in ensuring the inclusion of only the desirable contributions from the short-lived resonances. The final working relation here, thus, boils down to

$$\langle f \rangle(p_T, Y) = \sqrt{\lambda} \frac{dN}{dY dM_T dM_T d\phi} \frac{1}{V_{\text{eff}}(p_T, Y)}. \quad (17)$$

3 Models for transverse one-particle spectra

The one-particle momentum spectrum, determined as the space time integral of the emission function $S(x, p)$ is sensitive to the momentum distribution in $S(x, p)$ and thus allows to constrain essential parts of the collision dynamics. For the heavy-nucleus collisions we start in our approach by considering the rapidity integral transverse momentum spectrum. We assume, first, that only the direct ‘‘thermally’’ produced pions are produced and so modelled. Secondly, for the sake of simplifying the calculations, we neglect here the contributions arising out of the resonance decays — both short-lived and long-lived.

As was done by Humanic [8] let us take the one-particle transverse momentum spectra given by

$$\frac{dN}{M_T dM_T} = C \exp \left[-\frac{M_T}{\Delta} \right], \quad (18)$$

where $M_T = \sqrt{(p_T^2 + m^2)}$ is the transverse mass, p_T is the transverse momentum, m is the particle rest mass, C is a normalisation constant and Δ is the slope parameter. But the observations over the one-particle spectra reveal that the slopes appear systematically flatter for

central collisions than for peripheral ones [9]. The above parametrisation of one-particle spectrum is suitable only in the region $0.8 \text{ GeV}/c^2 \leq M_T \leq 2.0 \text{ GeV}/c^2$. The flattening of the distributions with increasing centrality shows that the spectral shapes can be described very poorly by an exponential curve. Actually, a concave behaviour of pp data is observed over the whole M_T range. Its properties can be analysed quite well by calculating the local slope, defined by

$$T_{\text{loc}}^{-1} = -\frac{d}{dM_T} \left[\log \left(E \frac{d^3\sigma}{dp^3} \right) \right]. \quad (19)$$

The observed local slopes are not constant, as in the case of a purely exponential distribution, but change continuously over the measured M_T range for both central and peripheral collisions. At high p_T , where the nucleus-nucleus collisions can be described by perturbative QCD, the pion production spectra show a power law behaviour. Hagedorn suggested a parametrisation for inclusive cross-sections in pp collisions in the following form [10]:

$$E \frac{d^3\sigma}{dp^3} = C' \left(\frac{p_0}{p_T + p_0} \right)^n, \quad (20)$$

where C' , p_0 and n are free parameters, which are presented in a tabular form (table 2 below). The longitudinal component of the inclusive cross-section reflected through the rapidity term or variable has been absorbed as nearly a constant in the empirical C' term. This renders the left-hand sides of both (18) and (20) essentially quite compatible and comparable in so far as the production of single-particle spectra is concerned.

In fact, our main objective here is to put these two empirical models for hadronisation (after freeze-out) to test and examine their validity in the light of the measurement of the observable, average phase space density.

For nucleus-nucleus collisions ($A+B$ collisions) the inclusive cross-section possesses a nuclear dependence term as follows [11, 12] :

$$E \frac{d^3\sigma}{dp^3} (AB) = (AB)^{\alpha(p_T)} E \frac{d^3\sigma}{dp^3} (pp). \quad (21)$$

The parameter $\alpha(p_T)$ depends weakly on rapidity but strongly on p_T . At low p_T , α increases and this indicates a growing participation of the nuclear volume. In the present work, neglecting rapidity links, we take $\alpha \sim 1 + 0.06p_T$ for lead-lead collisions and moderate values of $p_T \leq 3 \text{ GeV}/c$. The chosen expression for α as a function of transverse momentum is cast in the present form in order to give the inclusive cross-section results an interaction-specific dependence of form. The coefficient of transverse momentum in $\alpha(p_T)$, which varies quantitatively and slowly from reaction to reaction depending primarily on the mass numbers of both the projectile and target nuclei, takes care of this feature. We have so far an intuition and insight, supported by data available to us to date for some heavy nucleus-nucleus collisions, that the coefficient is dependent on the product of the mass numbers of the target and projectile

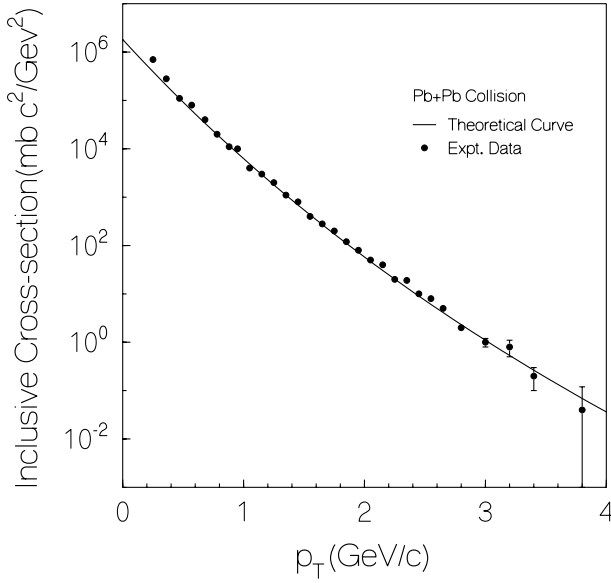


Fig. 1. Plot of $E \frac{d^3\sigma}{dp^3}$ versus p_T for pions produced in Pb-Pb reaction at CERN. Data points are from ref. [12].

nucleus. The nature of the dependence of the coefficient can be predicted/ascertained, if and only if the relevant data on a set of good number of nucleus-nucleus collisions at high energies involving nuclei of intermediate-range mass numbers are available. In this connection an interesting point of probe is whether the coefficient has any \sqrt{s} -dependence or not; though, for the sake of simplicity and due to paucity of data, which are available only for a very few and sparse specific center of mass energies, we have chosen temporarily not to broach here on this aspect in any further detail. In our opinion, it would be better to suggest tentatively a form of dependence, $\alpha(x_T)$, where $x_T = \frac{2p_T}{\sqrt{s_{NN}}}$ which would be much more consistent and compatible with the idea of the scaling. We have a plan to work on this problem with this approach in a series of future work. However, for the present, let us proceed with the given simple form with a view to just reproducing the data successfully and as simply as possible, though, obviously, in a phenomenological manner. The further assumption here of linear dependence is for both simplifying the calculations and obtaining reliably good fits with various data-sets. Thus, seen from this angle of simple physics, for Pb-Pb collisions, the value of the coefficient is found to be 0.06. Besides, in the above choice we have introduced the probable role of the Cronin effect on the value of α considered here. The adjoining diagram (fig. 1) shows the nature of the very nice fit obtained by the combination of expressions (20) and (21) for the p_T spectra of pions produced in relativistic Pb-Pb collision. Data for Pb-Pb collision are obtained from ref. [12]. In examining the general validity of the expressions forwarded and utilised here for the conversions of the results on inclusive cross-section for pion production in nucleon-nucleon collisions (as proposed by Hagedorn-based model) to those in high-energy nucleus-nucleus reactions, we have checked the proposed relationships for various proton-induced and

(heavy)nucleus-involved interactions at high energies with encouraging success. In a subsequent and separate paper, we are going to report on and deal with these very interesting results in some detail. And on the basis of it a point must be made quite emphatically and that is: the observed excellent agreement between the newly proposed models and the data-sets on Pb-Pb reactions is just not fortuitous. The underlying physics seems to have much deeper significance and stronger basis which we would hint later. With this statement, let us now revert, once again, to the calculational procedure.

The theoretical estimate of the factor $\frac{dN}{M_T dM_T dY d\phi}$ in the final working formula (eq. (17)) has to be obtained on dividing eq. (21) by the total inelastic cross-section σ_{in} for $A + B$ collisions. Hence, the required expression is

$$\frac{dN}{M_T dM_T dY d\phi} = \frac{1}{\sigma_{in}} (A \cdot B)^{\alpha(p_T)} E \frac{d^3\sigma}{dp^3} (pp). \quad (22)$$

Therefore, the average phase space density, denoted by $\langle f_{Hag} \rangle$, using Hagedorn's expression (eq. (20)) for single-particle spectrum, is given by

$$\begin{aligned} \langle f_{Hag} \rangle &= \frac{1}{\sigma_{in}} E \frac{d^3\sigma}{dp^3} (A \cdot B) \\ &\times \frac{\sqrt{\lambda} \pi^{3/2}}{M_T \cosh Y R_s(p_T) \sqrt{R_o^2(p_T) R_l^2(p_T) - R_{ol}^4(p_T)}} \\ &= \frac{(A \cdot B)}{\sigma_{in}} C' \left(\frac{p_0}{p_T + p_0} \right)^n \\ &\times \frac{\sqrt{\lambda} \pi^{3/2}}{M_T \cosh Y R_s(p_T) \sqrt{R_o^2(p_T) R_l^2(p_T) - R_{ol}^4(p_T)}}. \quad (23) \end{aligned}$$

To compare $\langle f_{Hag} \rangle$ with the average phase space density derived from an exponential distribution of single-particle spectrum, we also calculate the APSD by adopting Humanic's model [6]. And the expression for APSD from Humanic's model is given by

$$\begin{aligned} \langle f_{Hum} \rangle &= \frac{C \sqrt{\lambda \pi}}{2} \\ &\times \frac{\frac{dn^-}{dy} \exp[-M_T/\Delta]}{M_T \cosh Y R_s(p_T) \sqrt{R_o^2(p_T) R_l^2(p_T) - R_{ol}^4(p_T)}}. \quad (24) \end{aligned}$$

4 Inputs for calculation

In both cases the analyses here are done in the longitudinally comoving system (LCMS), where the longitudinal momentum of the pion pair vanishes. The HBT radii in LCMS are given by

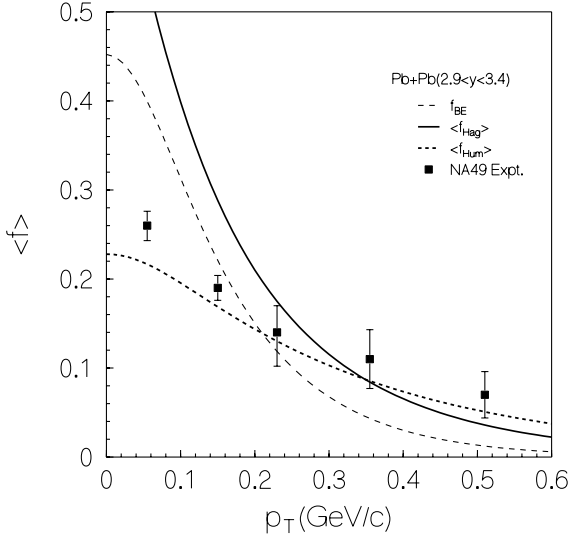


Fig. 2. Average freeze-out phase space density for Pb-Pb collisions as a function of p_T in the rapidity interval $2.9 < y < 3.4$. Data points are from ref. [2] and for $T = 120$ MeV.

Table 1.

T	η_f	R	τ_0	$\delta\tau$	$\delta\eta$	β_T
120 MeV	0.48	6.8 fm	8 fm/c	3.5 fm/c	1.3	0.7

Table 2.

C' (mb)	p_0 (GeV/c)	n	$A = B$
42	4.9	34	208

$$\begin{aligned}
 R_1^2(M_T) &= \tau_0^2 (T/M_T), \\
 R_s^2(M_T) &= \frac{R^2}{1 + (M_T/T) \eta_f^2}, \\
 R_o^2(M_T) &= R_s^2(M_T) + \frac{1}{2} \left(\frac{T}{M_T} \right)^2 \beta_T^2 \tau_0^2, \\
 R_{ol}^2(M_T) &= \frac{p_T Y}{M_T^2} \frac{T}{(\delta\eta)^2} \left[(\delta\tau)^2 + \tau_0^2 \frac{T}{M_T} \right], \quad (25)
 \end{aligned}$$

where τ_0 is the longitudinal proper freeze-out time, $\eta = \frac{1}{2} \ln \frac{t+z}{t-z}$ is the space time rapidity, η_f is the transverse flow strength of the source and $R = R(\text{Pb}) = 1.15 \times (208)^{1/3} = 6.8$ fm with Woods-Saxon density distribution [13].

The values of different source parameters used in our calculation are given in table 1.

In Hagedorn's model for pionisation the parameters are given in table 2.

In Humanic's model the slope parameter is given by $\Delta = 270$ MeV. The value of λ in both the cases was taken 0.7. The overall analyses were done separately for three regions of two-particle rapidity bins of width 0.5.

The results of our calculations based on both Humanic's as well as Hagedorn's models for pionisation are

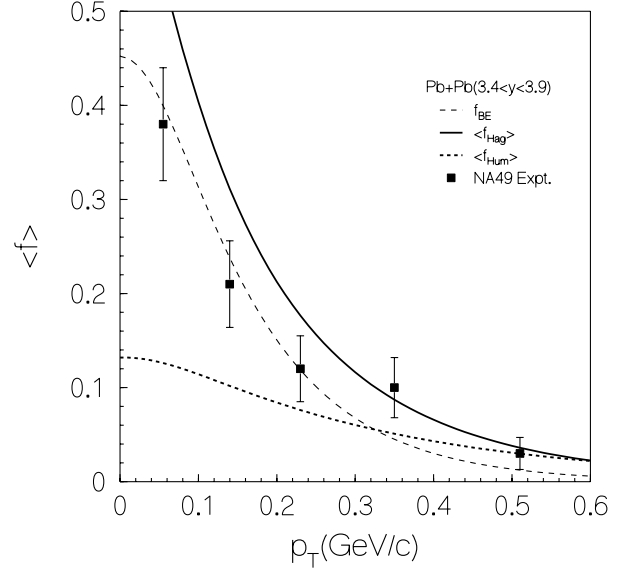


Fig. 3. Average freeze-out phase space density for Pb-Pb collisions as a function of p_T in the rapidity interval $3.4 < y < 3.9$. Data points are from ref. [2] and for $T = 120$ MeV.

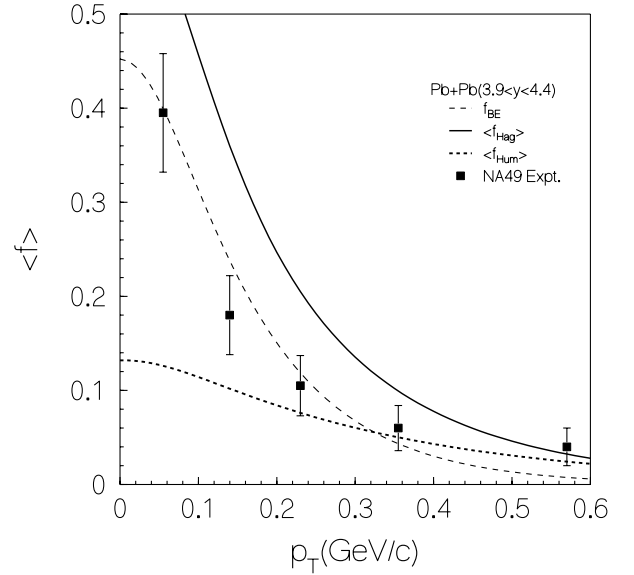


Fig. 4. Average freeze-out phase space density for Pb-Pb collisions as a function of p_T in the rapidity interval $3.9 < y < 4.4$. Data points are from ref. [2] and for $T = 120$ MeV.

presented in fig. 2 to fig. 4. They have also been compared with the experimental measurements indicated by filled squares and also with the results of the thermal model represented here by the Bose-Einstein equilibrium distribution and depicted in the graphs by the dotted curves.

5 Results and discussion

The adjoining diagrams (fig. 2 to fig. 4) demonstrate here the performances of the chosen phenomenological models for pionisation after freeze-out. The thin dashed curves

represent the status of the thermal model with regard to the estimation of the APSD; the relatively thick dashed curves provide the fit at $T = 120$ MeV based on Humanic's model [8] which assumes an exponential transverse momentum distribution for pions, and the solid curves (present work) in the figures depict the calculations for the same on the basis of Hagedorn's model. The comparison of the diagrams shows that Humanic's model describes quite well the data in the rapidity region, $2.9 < y < 3.4$, but fails for the other higher rapidity windows; whereas on APSD the other two models perform somewhat better in comparison, especially in the rapidity window, $3.4 < y < 3.9$. However, in the rest of the present discussion, we will keep ourselves confined only to the thermal and the Hagedorn's model, as firstly, the thermal model constitutes predominantly the state-of-the-art approach and, secondly, Humanic's model, until now, is not a very widely applied model. It is also undeniably true that, in so far as the application of Hagedorn's model to the issue of average phase space density in heavy-ion collisions is concerned, the approach offered by us here is somewhat in the same position as that of Humanic's one. Still, the search for a new and better approach is always justifiable in physics, in particular and in science, in general.

Hagedorn's model used here, quite notably, smacks essentially of the idea of Feynman scaling, as the inclusive cross-section is assumed to behave in an energy-independent manner and it is quite well known that from small to modestly high p_T ($p_T \leq 2$ GeV/c) region even the QCD-inspired jet models prescribe only moderate and no strict observance of the Feynman scaling. Thus, it is hardly surprising that the Hagedorn's model with modest observation of the Feynman scaling provides a good description of the data on APSD and that could be set, in our opinion, on a par with the thermal model which is surely a phenomenological model.

The calculations are made here by us for Pb-Pb collision alone and for hypothetical freeze-out temperature ($T = 120$ MeV), as the data are available only for $T = 120$ MeV. Besides, we have also tested the present approach with the estimation of APSD factor for some other sulphur-induced heavy-ion reactions with remarkable success which we had dealt with in a separate work [14]. The modest agreement for Pb-Pb collision has been obtained here for a wide region of the transverse momentum spectra with Hagedorn's model and with temperature value of $T = 120$ MeV. Agreement with data is reasonably fair for the intermediate range of p_T values. And this is only natural as the measurements at very small p_T values ($p_T \rightarrow 0$) or at very large p_T values are always liable to errors. Finally, our calculation-based diagrams, which depict the general nature of the APSD factor and its values at various transverse momenta, corroborate consistently the observed physical features of pionisation in the relativistic lead-lead collisions. So, in our opinion, the new approach induced by the application of Hagedorn's model for nucleus-nucleus collision might provide either a par-

allel or a viable alternative to the set of the few existing models.

6 Concluding remarks

Let us now sum up the main observations made here. The calculational support to the QCD-inspired description of the particles produced in high-energy collisions in the prescription offered by Hagedorn is quite evident from the nature of agreement between data and calculations. The present study produces a fit to the observed data somewhat comparable to the thermal model with Bose-Einstein distribution for, at least, some of the heavy-ion collisions. Hagedorn's model is an indirect and implicit hint to accept the Feynman scaling (even if that be for a particular small range and region for p_T values) as a reasonably solid plank. And, to our mind, this worked quite well in so far as the estimation of the average phase space density in Pb-Pb collision at 158A GeV/c and of some other heavy-ion reactions as well is concerned. A point must be made here. The models under consideration in the present work have peculiarly a common feature in the fact that all of them provide perceptibly better fits to the data for rapidity y -values in the range $3.4 < y < 3.9$, though we fail to provide any tangible explanation for such observations.

Prior to the present work, we have utilised the foundational hypothesis of the present work to analyse the various proposed signatures of quark-gluon plasma (QGP) hypothesis with a modest degree of success. On the basis of this alternative approach we have calculated the ratios of kaon-pion [15], baryon-antibaryon and have compared the computed values with actual measurements. Such studies revealed striking agreement between measured data and calculations. All this simply reinforced and strengthened the basic premise of the present work which, stated simply, is: the physics of nucleon-nucleon collisions, at very high energies, might be of some relevance to understand the physics of high-energy heavy-ion collisions.

The authors would like to express their thankful gratitude to the learned and anonymous referee for some helpful comments and valuable suggestions. It is also a great pleasure on their part to thank Drs. P. Seyboth, D. Rohrlich, T. Peitzmann and E. Garcia-Solis of various Collaborations for some very kind and prompt electronic correspondences at personal level, while the work was in progress. Mr. P. Guptaroy of IACS, Calcutta-700032 is also thanked for his continuous technical help and encouragement.

References

1. A. Wagner et al., Phys. Rev. Lett. **85**, 18 (2000).
2. D. Ferenc et al., Phys. Lett. B **457**, 347 (1999).
3. D. Ferenc, B. Tomasik, U. Heinz, preprint CERN-TH/99-14.
4. B. Tomasik, U.A. Wiedemann, U. Heinz, preprint CERN-TH/99-215, July 1999.

5. U.A. Widemann, U. Heinz, Phys. Rep. **319**, 145 (1999).
6. G.F. Bertsch, Phys. Rev. Lett. **72**, 2349 (1994).
7. G.F. Bertsch, Phys. Rev. E **77**, 789 (1996).
8. T.J. Humanic, Phys. Rev. C **60**, 014901 (1999).
9. WA80 Collaboration (R. Albrecht et al.), Eur. Phys. J. C **5**, 255 (1998).
10. R. Hagedorn, Riv. Nuovo Cimento **6**, No. 10 (1983).
11. T. Peitzmann, Phys. Lett. B **450**, 7 (1999).
12. T. Peitzmann, <http://alice.web.cern.ch/Alice/qm97/peitzmann/index.html>.
13. NA49 Collaboration (H. Appelshäuser et al.), Eur. Phys. J. C **2**, 661 (1998).
14. S. Bhattacharyya, Bhaskar De, preprint PAMU/ISI-2000.
15. S. Bhattacharyya et al., Hadronic J. Suppl. **15**, 451 (2000).